JOURNAL OF SYNCHROTRON RADIATION

Volume 27 (2020)

Supporting information for article:

Versatile Compact Heater Design for *In Situ* Nano-Tomography by Transmission X-ray Microscopy

Stephen Antonelli, Arthur Ronne, Insung Han, Mingyuan Ge, Bobby Layne, Ashwin Shahani, Kazuhiro Iwamatsu, James F. Wishart, Steven Hulbert, Wah-Keat Lee, Yu-chen Karen Chen-Wiegart and Xianghui Xiao

S1. Engineering Design Details on the *In Situ* Heater

In a TXM configuration, there is always a pinhole upstream of the sample to block the direct beam leaking through the condenser. The pinhole position has to be very close to the sample position. The copper casing is 30 mm in diameter. Two flat surfaces were cut on the upstream and downstream sides of the copper casing to make more room for the upstream and downstream optics.

The heating wire was wound on a standard M6x1 threaded rod to produce a single helix with an inner diameter of approximately 5.5 mm, approximate pitch of 1 mm, and overall resistance of 1.9 ohm. The core pin assembly was comprised of an aluminum rod of diameter 5 mm machined with small cross-holes into which precision tool-steel rods were inserted. The configuration and size of these seven cross holes were matched to the horizontal plane penetrations in the heater casing: two φ1mm holes for the X-ray beam entrance and exit, a φ2mm hole for the side-view camera for viewing the sample, and four φ1.6mm holes for general purpose input/output, one of which was to be dedicated for the placement of the temperature sensor providing feedback signal to the temperature controller. The horizontal cross-pins were then inserted, the wire was carefully bent around the cross-pin configuration, and finally returned to the M6 threaded rod to complete the winding of the second half of the helix. The two leads of the wire were bent at 90-degree angles so they could exit the heater casing and trimmed to length.

In the interest of protecting the neighboring TXM optics, an estimation was made for the heat radiated from a 1100 ºC furnace core to a neighboring optic at R = 12 mm away. Assuming the shape factor formed by a point source (sample) projected through a φ1 mm x-ray beam aperture at a radius of 10.5 mm (equation 1a) and an ambient temperature of 25 ºC, Equation 1b was used to estimate a <1 mW heat transfer. This heat transfer was assumed to be tolerable by the neighboring optics, however, mechanical features were designed into the furnace casing to allow a thin metal foil heat shield to be clamped against the water-cooled casing on the beam entrance and exit apertures if needed.

Shape Factor: $F = \frac{D^2}{4R^2+D^2}$

Radiation Heat Transfer: $q = \sigma AF({T_{furnace}}^4 - {T_\infty}^4)$ The furnace takes a cylindrical form factor with a 31 mm overall height and a clear φ5 mm inner bore through the center of the heater coil. The casing is constructed from two mirror-image "C-shaped" halves which are pinned and bolted together. Seven different penetrations radially distributed through the casing in the horizontal plane (sample plane) allow passageways for the incoming and outgoing X-ray beam, visual access for the side-facing camera, as well as onboard temperature sensor placement. Some of these penetrations are reserved as "spares" to allow future-scope capabilities such as onboard transmissive and reflective fiberoptic

illumination of the sample. Φ0.125" copper tubes formed into a "U" shape are brazed to each half of the furnace, and ultimately connected in series via push-to-connect unions and Φ0.125" Nylon tubing to form one continuous cooling loop. The two-part separable design is thought to facilitate the assembly and maintenance (e.g. replacing heater coils) through the operating lifetime. OFHC Copper cover plates are fastened to the top and bottom of the casing. They serve as an additional means of fastening the casing together and consequently provide indirect cooling to the top and bottom surfaces of the heater coil. A φ5 mm aperture in the bottom cover plate aligns with the coil aperture and allows the sample to be inserted into the center of the furnace. For samples that are longer than the length of the furnace, an identical cover plate may be used on the top to allow the top end of the sample configuration to exit the top of the furnace. For shorter samples, the solid top cover plate may be used, or the hole can be plugged with ceramic wool. This is believed to yield slight gains in both thermal performance and uniformity of the inner heating zone.

Implementation on the TXM instrument was realized via a custom XYZ stepper-motor positioning system (Figure S1C). At the end of the positioning system is a φ12.7 mm clamp holder with manual rX and rY adjustments. A 304 stainless steel adapter bracket is attached to the side of the furnace and connected to a standard φ12.7 mm optical post that is clamped by the positioning system. Future versions of this adapter bracket are recommended to be constructed from G-10 plate to provide an extra layer of electrical and thermal isolation between the furnace casing and the environment. This connection and support method allow the furnace to be remotely raised and lowered (Y axis) and adjusted laterally (X and Z axes) about the sample. It also allows for scanning experiments, e.g. characterization of inner heating zone. However, in general, the minimum hardware needed to support the furnace is a standard φ12.7 mm optical post clamp.

The furnace utilizes a heating element comprised of a resistive heater coil embedded within a ceramic insulating shell. The wire material used for the coil is Kanthal® A-1, an FeCrAl alloy, 22AWG (.0253" diameter). The ceramic material is Aremco Ceramacast™ 510, a cement-like Al_2O_3 power, and was mixed with room-temperature distilled water in a 20-to-3.8 ratio and poured around the naked coil while held in a cylindrical mold with an inner core-pin assembly. This method produces a cylindrically-shaped, integral ceramic-insulated coil with the well-controlled outer diameter, inner diameter, and horizontal plane penetrations.

The heater coil is powered by a Sorensen XG33-25 programmable DC power supply and controlled by a Lakeshore 336 temperature controller. High-temperature extension wires (Omega Item# HTMG-1CU-322S/C) provide a low-resistance connection between the heater coil and the power supply. All-metal crimp spade terminals are used to make the connection to the power supply, while custom-made Macor® ceramic barrel connectors with a single M2x0.4 set screw are used to lap and secure the extension wire to the coil leads. These ceramic connectors provide two necessary functions; a high-temperature resistance to withstand the heat transferred to the extension wire by the heater coil, and a

layer of electrical isolation between the heater coil wire and the environment. However, the Macor® ceramic is a brittle material and the small threads in this connector tend to fail under relatively low stresses. This is a recommended area for improvement in future design revisions.

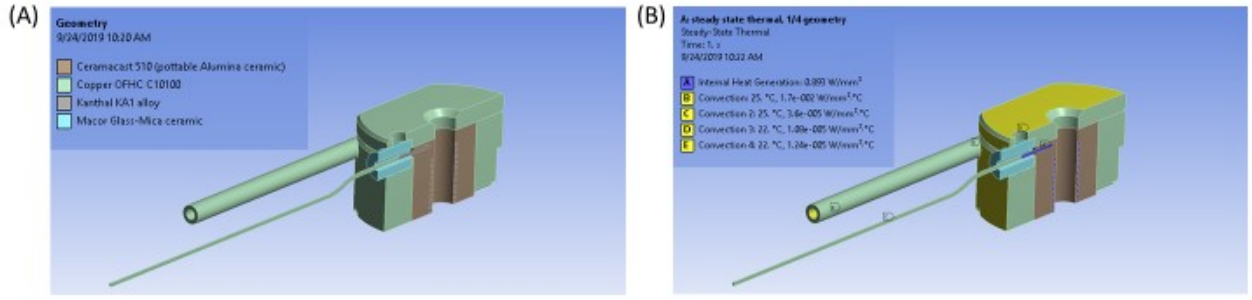

Figure S1. A steady-state thermal Finite Element model of the furnace assembly was constructed with ¼ symmetry.

Tabulated thermal properties for OFHC copper were assigned to the furnace casing and the cooling tube bodies. Manufacturer data for the Kanthal® A-1 wire, Ceramacast™ 510, and Macor® materials were consulted and subsequently incorporated into the model. A coil with a total length of ~385 mm was assumed, and the overall resistance was estimated to be 1.72 ohm. Assuming a power supply of 24 VDC, a total power dissipation of ~334 W was calculated. A volumetric heat load was calculated by dividing the total power dissipation by the total coil volume and then applied to the coil body in the model, however one aim of the FEA model was to study the effect of this parameter on the maximum temperatures within the furnace constituents.

Next, contact conditions were established between the various solid bodies within the model. The contacts were divided into three categories – “perfect” thermal contacts, “reasonably good” thermal contacts, and “poor" thermal contacts. The first category was used to simulate brazed connections and in places where a worst-case thermal result was desired, e.g. heat transferred to extension wire via heater coil. A value of .01 W/mm^2K was used for “reasonably good” contacts and applied to areas where heat removal was desired, such as the bolted copper-to-copper interfaces between the heater cover plate and the water-cooled furnace casing. A value of 0.001 W/mm^2K was used for “poor” thermal contacts and applied to areas were poor thermal contacts were anticipated, e.g. between the outside of the heater coil’s ceramic shell and the inside of the copper casing.

Convection boundary conditions were selected and applied to the inner surfaces of the cooling tube and the outer surfaces of the furnace casing to try and capture a realistic grouping of heat sinks. A flowrate of 0.25 GPM and bulk fluid temperature of 25 ^{o}C was used to calculate an initial convection

coefficient of .035 W/mm^{2}K on the inner cooling tube surface, however this parameter was also varied in the study. Free convection coefficients between 1.1e^{-5} and 3.6e^{-5} W/mm^{2}K were applied to vertical, horizontal up-facing and horizontal down-facing surfaces assuming an ambient air temperature of 25 ºC. The results of the study can be seen in the main manuscript. This study demonstrated the potential for the furnace to reach the target inner temperature of approximately 1100 ºC and suggested that the optimal range of power dissipation and coolant flow rate were in the vicinity of 125 W and between 0.1 and 0.5 GPM, respectively.

In addition, an analytical calculation was conducted to determine the power supply and cooling water flowrate requirements for the heater to reach the targeted temperature at the heating coil [Figure S2(a)] while keeping the casing at near room temperature [Figure S2(b)].

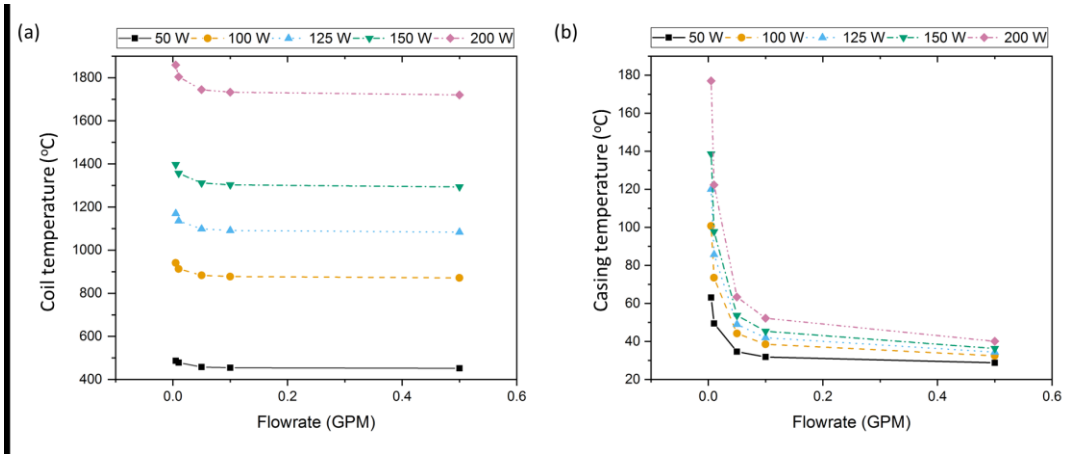

Figure S2. Analytical analysis to determine the adequate power supply (a) and cooling water flowrate (b).

Initial testing of the heater was performed in a laboratory setting with no closed-loop temperature control. The experimental setup is pictured in Figure S3. The water-cooling was delivered by a ThermoFlex 900 air-cooled recirculating chiller. A regulating valve and flowmeter were plumbed into the cooling loop to provide precision flow control and monitoring. The heater was powered by the Sorensen PSU in control voltage mode – this involved establishing a voltage setpoint and a maximum current limit. The resulting current draw was determined by the electrical load. Care was taken to verify the coil resistance and electrical isolation between the coil leads and the outer furnace components (casing, cover plates, tubing, etc.) prior to energizing the coil. The proportional–integral–derivative (PID) parameters for the power supply were tuned before the tests. The coil was tested at several voltage setpoints while the current draw and temperatures in three key locations were recorded; the inner coil surface (which later would be the sensor location for in-situ temperature control), the sample location, and the outer surface of the casing. K-type thermocouples were used to make all temperature measurements. Initial tests demonstrated the ability of the furnace to reach the target 1100 ºC easily while dissipating approximately 240 W. Deviations between this measurement

and the FEA model prediction are suspected to be due to the realization of a far more efficient cooling scheme than what was assumed in the model. It also demonstrated a seemingly high level of temperature stability and repeatability. Initial testing suggested that optimal coolant parameters were 0.25 GPM and 25 ºC. An observed rise time of >1000 ºC/min when subject to a 0-to-20 V step change and fall time of ~200 ºC/min indicated usefulness for both heating and quenching applications.

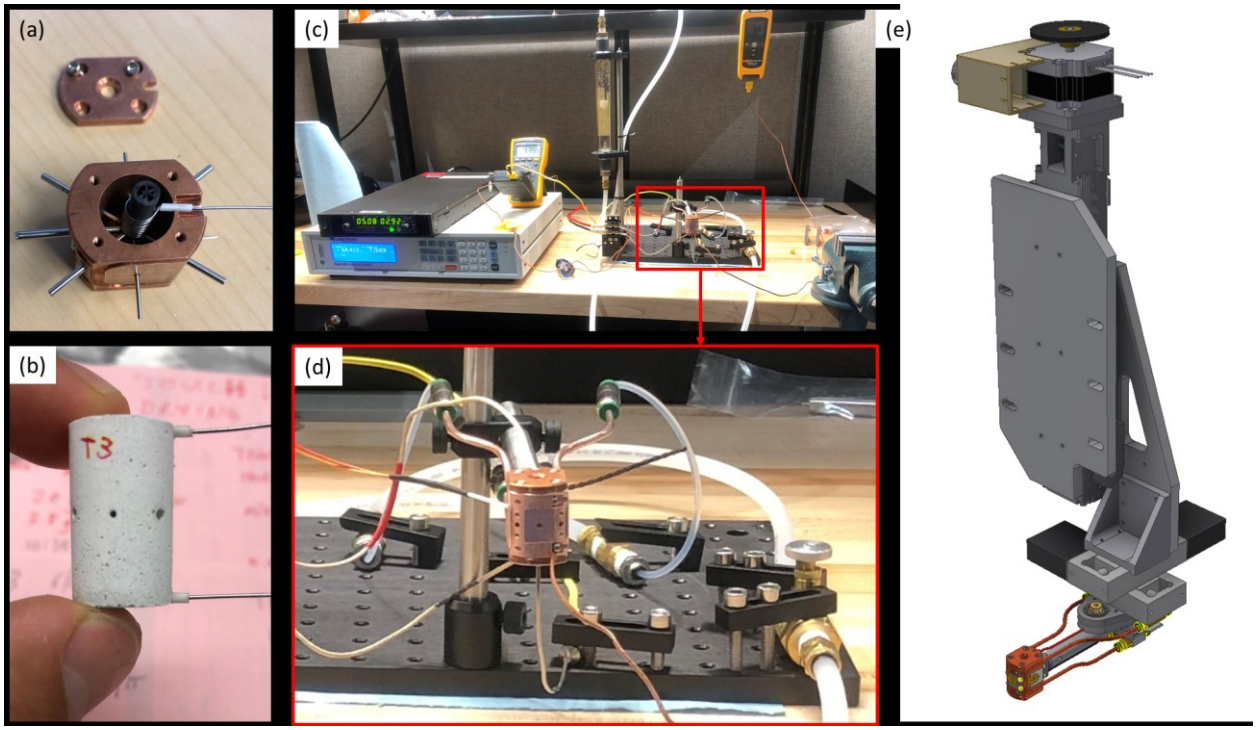

Figure S3 . (a-b) Additional details for the structure of the core-pin assembly. (c-d) Furnace testing in a laboratory setting. (e) the mounting of the heater to an x-y-z stage stack designed to align the heater at the beamline.

S2. Salt preparation, TXM sample preparation and TXM measurements for the molten salt application

S2.1 Salt Preparation

Solid magnesium chloride ($MgCl_2$) was purified using a distillation chamber that consisted of a heated zone and a cold zone. The $MgCl_2$ was first loaded into one side of the distillation column which was heated to 925 °C while under a constant vacuum of $1x10^{-3}$ Torr. Over time, the pure $MgCl_2$ evaporated from the heated zone and condensed in the cold zone leaving any contaminants in the heated zone. This anhydrous $MgCl_2$ was mixed in a 50:50 molar mixture with as-received anhydrous KCl salt (99.9%) (Sigma-Aldrich- 449989) and ground together in a mortar and pestle in a glovebox.

S2.2 TXM Sample Preparation

Nickel alloy wire containing 20% chromium (Ni-20Cr, 99.5% pure) with a diameter of 20 μm (Goodfellow, USA- NI055105) was used for this study. The wire was used "as-drawn", meaning that no annealing was done after the wire was drawn through a diamond die. Microwires are ideal materials for study in X-ray nano-tomography as the cylindrical shape allows for consistent X-ray attenuation; the diameter of 20 μm was chosen based upon the need to ensure both sufficient X-ray transmission, and an adequate size for the field of view. This wire was inserted into the end of a 0.1 mm diameter quartz capillary (Charles Supper) and transferred into the glovebox. Inside the glovebox, these wire-filled 0.1 mm diameter quartz capillaries along with 1.0 mm diameter quartz capillaries were baked out at approximately 200 ºC for at least three hours to remove residual moisture adsorbed on the surface of the quartz capillaries. In a quartz boat, the salt mixture was heated to 550 ºC to allow for melting. A syringe was attached to end of the wire-filled 0.1 mm capillary and sealed using parafilm, the capillary was dipped into the molten salt mixture and the plunger of the syringe was drawn back to draw up the molten mixture. The salt mixture solidified almost immediately upon drawing up. The now salt-filled, wire-filled 0.1 diameter quartz capillary was broken to a length of ~ 10 mm and then placed into the 1.0 mm diameter capillary. The top of the 1.0 mm diameter capillary was epoxy-sealed and allowed to cure for at least 2 hours within the glovebox. The samples were then transferred out from the glovebox. The capillaries were then sealed with flame using a hydrogen mini-torch and mounted onto sample holders for the transmission X-ray microscope.

S2.3 TXM measurements

The Ni-20Cr sample immersed in 50:50 molar KCl:$MgCl_2$ was heated in the *in situ* furnace to 800 ºC at a ramp rate of 25 ºC/min, and held at that temperature for four hours, then cooled back to room temperature with a ramp rate of 50 ºC/min. The corrosion of the wire was observed *in situ* using X-ray nano-tomography at 8.33 keV. The energy was chosen to be just slightly below the Ni absorption K-edge of 8.333 keV for optimal contrast. A lens-coupled CCD detector with 2560 (h) x 2160 (v) pixels was used, with a field of view of ~55.5 x 46.8 μm^2. A camera binning of 2 x 2 was used, resulting an effective pixel size of 43.34 nm. For each tomography measurement, approximately 1050 projections were collected with an exposure time of 50 ms, and a total acquisition time of 2-2.5 min per scan. Tomography scans were collected continuously during isothermal heat treatment of microwires in the molten salt. The tomography reconstructions were done with Tomopy, an open source tomographic data processing toolbox (Gursoy *et al.*, 2014). The projection images were low-pass filtered before the tomography reconstructions with the gridrec algorithm(Dowd *et al.*, 1999, Rivers, 2012).

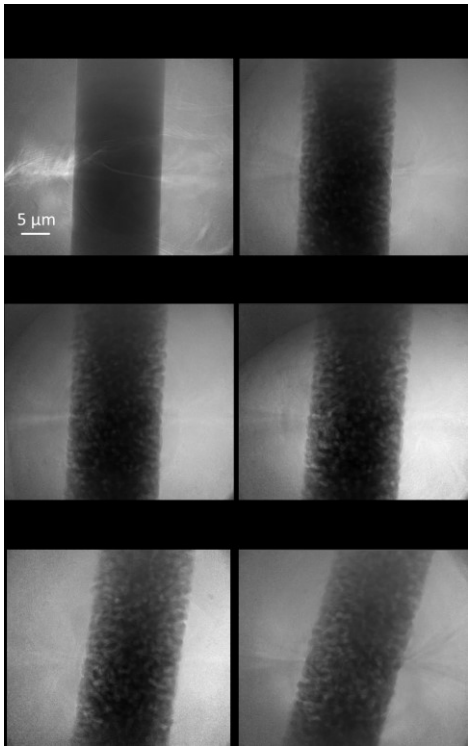

Figure S4. Transmission X-ray microscopy projection images showing the structural evolution of the Ni-20Cr wire in the first 16 minutes at 800 °C

S3. Further details for quasicrystals applications

During the *in situ* heating at 800 °C, the sample was continuously rotated at 3 °/s with 100 ms exposure time per each projection image. The X-ray energy was set to 8.34 keV and the images were acquired with 2 × 2 binning, resulting in a pixel size of 42.8 nm × 42.8 nm.

Estimation of vacancy supersaturation S of thermal vacancies in quasicrystals

The thermal vacancy supersaturation **S** can be represented as the following equation,

$$\mathbf{S} = \mathbf{exp}\left[\frac{-\Delta\mathbf{H_f}\left(\left(\frac{\mathbf{1}}{\mathbf{T_m}}\right) - \left(\frac{\mathbf{1}}{\mathbf{T}}\right)\right)}{\mathbf{k}}\right]$$

where $\mathbf{\Delta H_f}$ is the enthalpy of vacancy formation (2.3 eV (Sato *et al.*, 2003)), $\mathbf{T_m}$ is the melting temperature of the icosahedral Al-Pd-Mn QC phase (890 °C (Dovbenko *et al.*, 2005)), and **k** is the Boltzmann constant. At 800 °C, we find $\mathbf{S} = 6.85$, indicating a substantial chemical driving force to nucleate vacancy clusters.

References:

Dovbenko, O., Velikanova, T. & Balanetskyy, S. (2005). *Ternary Alloy Systems. Phase Diagrams, Crystallographic and Thermodynamic Data Critically Evaluated by MSIT. Group IV: Physical Chemistry. Subvolume A–Light Metal Systems*.

Dowd, B. A., Campbell, G. H., Marr, R. B., Nagarkar, V., Tipnis, S., Axe, L. & Siddons, D. P. (1999). *Conference on Developments in X-Ray Tomography II*, pp. 224-236. Denver, Co

Gursoy, D., De Carlo, F., Xiao, X. H. & Jacobsen, C. (2014). *Journal of Synchrotron Radiation* **21**, 1188-1193.

Rivers, M. L. (2012). *Conference on Developments in X-Ray Tomography VIII*. San Diego, CA

Sato, K., Baier, F., Rempel, A. A., Sprengel, W. & Schaefer, H. E. (2003). *Physical Review B* **68**.